Copy of: Proc. IEEE 1997 Int. Conference on Microelectronic Test Structures, Vol.10, March 1997

Determination of Defect Size Distributions Based on Electrical Measurements at a Novel Harp Test Structure

Christopher Hess, Larg H. Weiland

Institute of Computer Design and Fault Tolerance (Prof. Dr. D. Schmid)
University of Karlsruhe, P. O. Box 6980, 76128 Karlsruhe, Germany
Phone: +49-721-6084217; FAX: +49-721-370455; http://goethe.ira.uka.de/ddg

Abstract — **To improve accuracy of electrically based measurements of defect densities and defect size distributions, we present a novel harp test structure. There, horizontal and vertical parallel lines will be placed inside a given boundary pad frame without using any additional active semiconductor devices. The enhanced 2D-permutation sequence provides that all neighborhood relationships of adjacent test structure lines are unique. This is the key to disentangle even multiple faults detected by fast digital measurements. For this reason, the number and size of individual defects will be extracted anywhere inside or in-between layers.**

1 Introduction

Information about defect density and defect size distribution is important to control and optimize the manufacturing of integrated circuits. Especially defect size distributions are essential in accurate yield prediction [StRo95], [Ferr85c], [Maly90], [Stap84]. One common way to get data about defects is using laser scattering systems after selected process steps [TBG95]. But, not every detected particle defect results in an electrically measurable fault [HWLH96]. Therefore, it is important to determine a defect density based on the layout region of chips. Furthermore there are defects that are to small to become an electrically measurable fault. So, also test structures have to be used to get accurate data about the density and size distribution of defects that results in electrically measurable faults. A test chip without active semiconductor devices was introduced by [BCKJ91] to measure not just defect densities but also defect sizes. But the complex analog measurement procedure requires a constant sheet resistance per layer and also, disentangling of multiple faults is practically impossible.

So, we decide to develop a test structure to improve accuracy of densities and size distributions of defects based on digital electrical measurements only. The following Section describes the design principle of the novel harp test structure. Section 3 deals with the digital measurement procedure and the defect detection technics. Section 4 presents the methodology to determine a layer-sensitive defect size distribution based on the electrical measurements only. Section 5 gives some experimental results and finally we conclude our approach.

2 Design Principle of the Harp Test Structure

Parallel lines - each connected to an isolated pad - will be implemented inside a test structure to electrically determine a defect size distribution. If a defect occurs and causes an electrically measurable fault, two or more test structure lines will be shorted. The more test structure lines are connected, the larger the defect will be. The limitation of pads requires serpentine test structure lines to fill the complete test chip area [BCKJ91]. If more than two serpentine lines are connected, it is difficult to say whether there is just one large defect or some small defects have caused a multiple fault.

Short circuits will connect test structure lines if, and only if the lines are placed as neighbors anywhere inside the test chip area. So, the more different neighbored test structure lines will be implemented the more short circuits will be distinguishable which is important to disentangle multiple faults. So our goal is to increase the number of differently neighbored test structure lines without increasing the number of pads. The 2D-Permutation procedure introduced at [HeSt94] calculates a 2D-matrix just once containing all possible neighborhood relationships for **m** different index values.

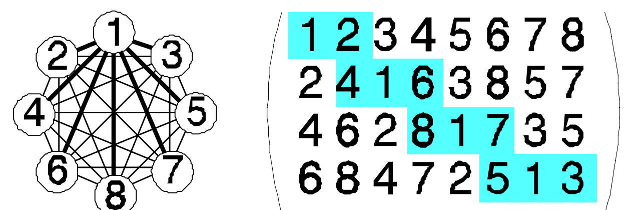

Fig. 1: Example of 2D-permutation procedure for **m=8** values.
Left: Complete neighborhood graph introduced by [HeWe94]:
nodes: Test structure lines connected to one pad.
edges: Two nodes are connected by an edge if test structure lines connected to these pads are adjacently placed anywhere inside a test chip with only nonconducting material between them.
Right: 2D-matrix, where the gray boxes mark pairs to line "1".

The following equation will be used to calculate the elements **a[i,j]** of the 2D-matrix, where the number **m** of used index values has to be even.

$$a[i,j] := \begin{cases} j + 2\cdot i - 2 & \text{where } \frac{j}{2} \in \mathbb{N} \quad \wedge\ i \le \frac{m - j - 2}{2} \\ 2\cdot m - j - 2\cdot i - 3 & \text{where } \frac{j}{2} \in \mathbb{N} \quad \wedge\ i > \frac{m - j + 2}{2} \\ 2\cdot i - j - 1 & \text{where } \frac{j+1}{2} \in \mathbb{N} \wedge\ i > \frac{j+1}{2} \\ j - 2\cdot i - 2 & \text{where } \frac{j+1}{2} \in \mathbb{N} \wedge\ i \le \frac{j+1}{2} \end{cases} \tag{1}$$

i,j : row index and column index of the 2D-matrix

Here we enhance the 2D-permutation procedure to get a unique sequence of test structure lines where each pair of adjacent lines exists once. The following Figure describes the so-called 2D-permutation sequence.

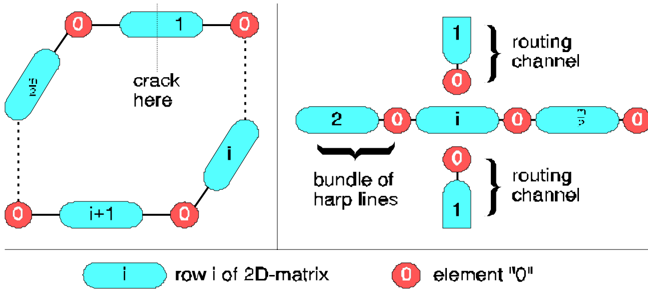

Fig. 2: 2D-permutation sequence.

In this sequence each row of the 2D-matrix will be implemented once. Furthermore, a new element will be added between these matrix rows. This additional element will be given the index value "**0**". In Figure 1 can be seen that each index value (**1 .. m**) of the 2D-permutation procedure exists just once in either the first matrix column (**j=1**) or the last matrix column (**j=m**). So, inside the 2D-permutation sequence, not only the neighborhood relationships inside the matrix rows are unique, but also all additional neighborhood relationships between the border elements of the matrix rows and the additional element "**0**". Just the number of index values - or the number $\mathbf{M_L}$ of pads inside a layer, respectively - increases to the odd value of **m+1** which will be required to design the 2D-permutation sequence. But, also the number of separable neighborhood relationships increases to ½·**m**·(**m**+1).

Now, the 2D-permutation sequence has to be transferred into a test structure design. For that we crack up the sequence within the first 2D-matrix row as can be seen in Figure 2. The elements of all matrix rows including the additional element "**0**" will be transferred into parallel test structure lines. The lines of the first matrix row will be designed vertical to all other lines to provide a routing channel. So, even defects may be evaluated that occur inside the routing channel.

This 2D-permutation sequence may be separately determined for each layer **L**. The lines inside each layer will be connected to a unique subset $\mathbf{M_L}$ of pads. The number of test structure lines per layer increases with the number of pads:

$$h_L := ½\cdot\left((M_L - 1)^2 + (M_L + 1)\right) \quad \text{where } M_L = m + 1 \ \wedge\ m \in \mathbb{N} \tag{2}$$

h_L : number of harp lines per layer inside the test structure
M_L : number of pads per layer

The following Figure 3 shows the principle design in two layers. The lower layer is filled with horizontal test structure lines and some vertical routing lines while vertical test structure lines and some horizontal routing lines are placed in the upper layer. The parallel arrangement of all these test structure lines inside a layer is responsible for the naming of the *harp test structure* where the subset of harp lines belonging to one matrix row including "**0**" is called a *harp bundle*. In Figure 3, all lines connected to the pads "1" and "7" are marked with bold lines. It can be seen that these two lines are adjacent once only - in the middle of the structure.

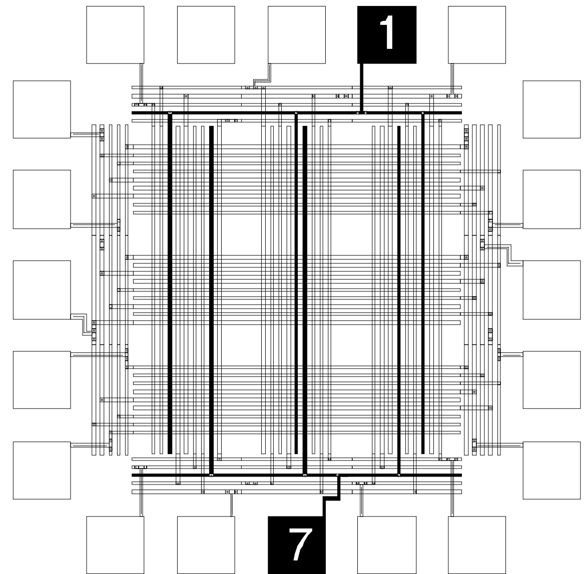

Fig. 3: Principle design of a two-layer harp test structure (HTS) connected to 2 * 9 pads of a 20 pad frame.

The 2D-permutation sequence guarantees this "*once-only-adjacent-condition*" for **all** implemented test structure lines and routing lines. Inside the harp test structure, not only all pairs of adjacent test structure lines are unique, but also **all** sets of more than two adjacent test structure lines are implemented once or none at all. This is the key to disentangle multiple faults. So, it is possible to conclude the size of defects from the number of adjacent test structure lines which are connected in case of a measured fault.

3 Measurements and Defect Detection

Generally, short circuits are detectable, testing the resistance between different pads or harp lines, respectively. To measure the resistance of the test structures, a digital tester will be used, because the electrical test must only decide whether there is a defect or not [HeWe95c]. The measured values are assigned to possible defects according to the following Table.

measured value		expected value in reference data	detected type of defect
voltage	binary		
$V_{measured} < V_{threshold}$	0	0	defectless
$V_{measured} < V_{threshold}$	1	0	short circuit

Tab. 1: Conversion of measured data.

If a defect occurs, two or more harp lines are connected to each other. The defect will be localized inside the harp test chip because each pair **(p,q)** of harp lines can be clearly assigned to a unique bundle index **i** and line index **j** inside the 2D-permutation sequence. Figure 4 contains the localization procedure for $\mathbf{0 \leq p < q \leq m}$, where **m** stands for the number of index values inside the 2D-matrix ($\mathbf{m=M_L-1}$). The flowchart uses the functions given in the following Table.

$$f(x) := \begin{cases} \frac{x}{2} & \text{if } \frac{x}{2} \in \mathbb{N} \wedge 1 < x \leq m \\ m - \left[\frac{x-1}{2}\right] & \text{if } \frac{x+1}{2} \in \mathbb{N} \wedge 1 \leq x < m \end{cases} \quad \mathbf{(3)}$$

$$F(x) := \begin{cases} 1 & \text{if } x = 1 \vee x = m \\ \frac{x}{2} + 1 & \text{if } \frac{x}{2} \in \mathbb{N} \wedge 1 < x < m \\ \frac{m}{2} - \left[\frac{x-1}{2}\right] - 1 & \text{if } \frac{x+1}{2} \in \mathbb{N} \wedge 1 < x < m \end{cases} \quad \mathbf{(4)}$$

$$g(x) := \begin{cases} ((x-1) \bmod m) - 1 & \text{if } x > 0 \\ (x \bmod m) - m & \text{if } x \leq 0 \end{cases} \quad \mathbf{(5)}$$

$$G(x) := \begin{cases} 0 & \text{if } x = 1 \vee 1<x<m \text{ where } \frac{x}{2} \in \mathbb{N} \\ m & \text{if } x = m \vee 1<x<m \text{ where } \frac{x+1}{2} \in \mathbb{N} \end{cases} \quad \mathbf{(6)}$$

Tab. 2: Functions used in the localization flowchart.

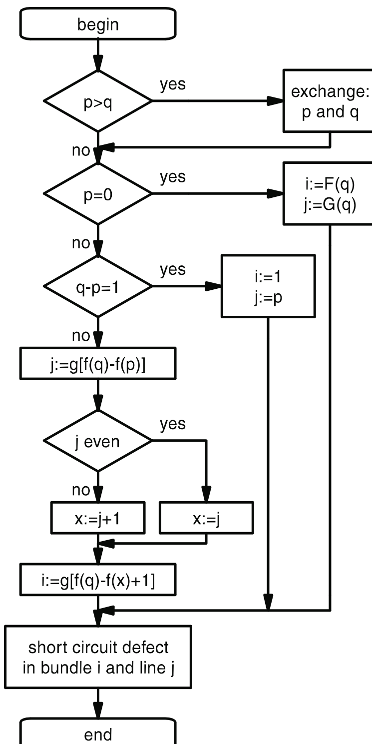

Fig. 4: Flowchart to localize defects.

If more than just two lines are connected, the following procedure will help to disentangle these multiple connection faults.

1. All possible harp line index pairs **(p,q)** will be extracted from the set of **k** connected pads in a short circuit.
2. The localization index **(i,j)** will be determined for each pair **(p,q)** of harp lines using the flowchart of Figure 4.
3. Then, subbundles of harp lines will be determined by combining those pairs $\mathbf{(p,q)_1}$ and $\mathbf{(p,q)_2}$ that have a common pad index and their localization indices meet:

$$\begin{aligned} & (\, i_1 = i_2 \quad \wedge \; |j_1 - j_2| = 1 \,) \\ \vee \; & (\, i_1 - i_2 = 1 \; \wedge \; (j_1 = 0 \wedge j_2 = m) \,) \\ \vee \; & (\, i_2 - i_1 = 1 \; \wedge \; (j_1 = m \wedge j_2 = 0) \,) \end{aligned} \quad \mathbf{(7)}$$

   If there is no further combination, each subbundle contains **n** harp lines that meet $\mathbf{2 \leq n \leq k}$.
4. Finally, we select the smallest number **d** of subbundles containing the indices of all **k** connected pads. So, **d** represents the minimum number of defects that have caused the measured multiple fault.

The following Figure 5 shows a harp test chip based on nine pads per layer containing a measured short circuit between **k=3** pads (indices: 1,3,7). So, there are three possible harp line index pairs (1,3), (1,7) and (3,7). Only the pairs (1,7) and (3,7) are adjacently placed as neighbors and may be combined in a subbundle that holds **n=3** pad indices (1,3,7). In this case, there is only one subbundle that contains all connected pads (**d=1**). More than 95% of all faults that connect more than just two pads may be summarized in just one "large" subbundle.

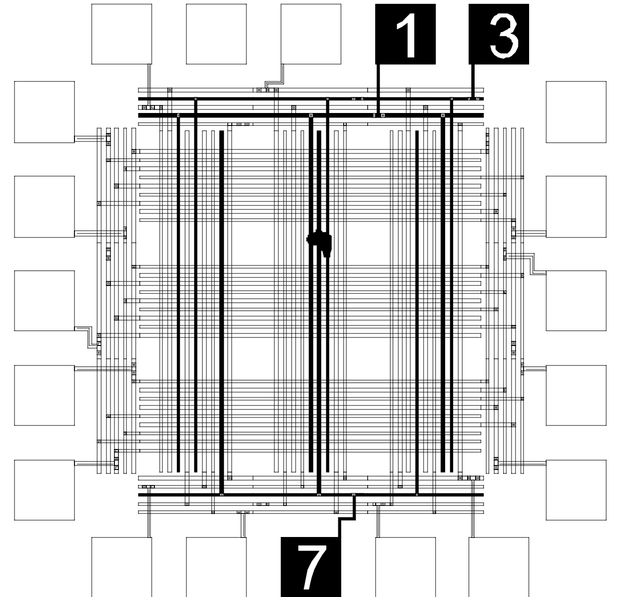

Fig. 5: Harp test structure containing a defect connecting 3 adjacent harp lines.

This analysis procedure leads to Figures showing the frequency of short circuit faults dependent on the number **n** of connected adjacent harp lines inside the subbundles. This is the key to calculate a defect size distribution based on the number of connected adjacent harp lines.

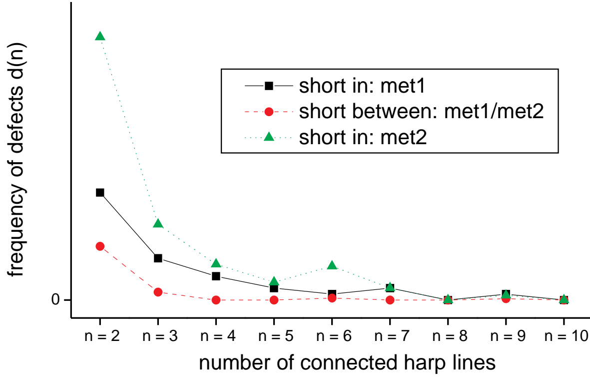

Fig. 6: Faults dependent on the number of adjacent harp lines.

4 Extraction of Defect Size Distribution

The number of connected adjacent harp lines has to be transferred to a size distribution dependent on the design rules of the harp lines. For that, the following Figure 7 shows some harp lines connected by defects. For a given line width **w** and space **s**, a defect that connects e. g. 2 harp lines may have a size in-between **s** and **s + 2·(w+s)**.

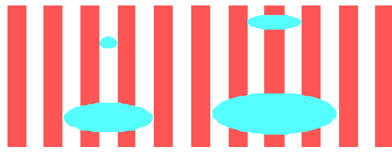

Fig. 7: Defects connecting 2 harp lines on the left side and defects connecting 3 harp lines on the right side.

So, a defect connecting **n** harp lines may have a size in-between the following *harp-interval* **HI(n)** where $n \in \mathbb{N} \wedge n \geq 2$:

$$HI(n) = [\, s+(n-2)\cdot(w+s)\,,\ s+n\cdot(w+s)\,] \tag{8}$$

The horizontal lines in the following Figure 8 represent the range of possible defect sizes (harp intervals **HI(n)**) for each number **n** of connected harp lines.

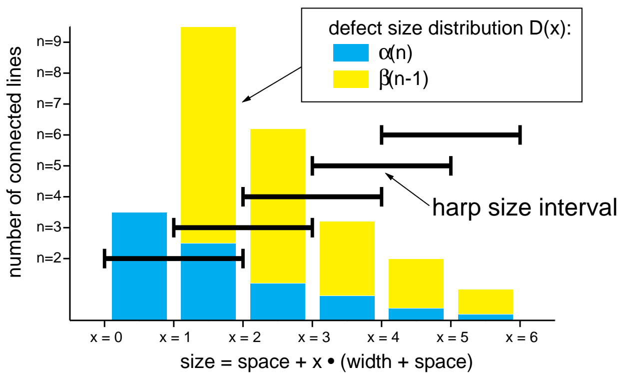

Fig. 8: Comparison of defect size intervals, where x = n - 2.

It can be seen, that there is an overlap between the different harp intervals. We have to summarize these overlapping intervals to get a size distribution. For that, we chose the following *size-intervals* **SI(x)** where $x \in \mathbb{N}_0$:

$$SI(x) := [\, s+x\cdot(w+s)\,,\ s+(x+1)\cdot(w+s)\,] \tag{9}$$

The frequency **d(n)** of all detected defects that connect exactly **n** harp lines has to be distributed among two size intervals. For that, we need **α(n)** defects transferred to the size interval **SI(x)** representing the smaller feature sizes and we need **β(n)** defects transferred to the size interval **SI(x+1)** representing the larger feature sizes, where:

$$\alpha(n)+\beta(n) = d(n) \quad \text{where} \quad n = x+2 \tag{10}$$

So, the number **D(x)** of defects inside each size-interval **SI(x)** will be:

$$D(x) = \alpha(x+2)+\beta(x+1) = \alpha(n)+\beta(n-1) \tag{11}$$

All these defect frequencies **D(x)** result in a size distribution illustrated as vertical bars in Figure 8, where also the fraction of α and β can be seen.

To determine the ratio of **α(n) / β(n)** we use the fault probability kernels introduced by Stapper [Stap84] and Ferris Prabhu [Ferr85c] as can be seen in the following Figure.

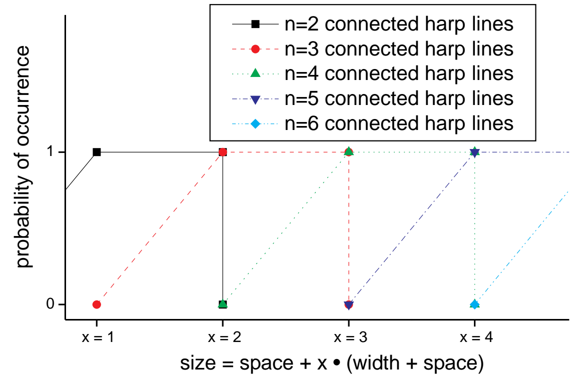

Fig. 9: Fault probability kernels of connected harp lines.

The probability that a defect within the size interval **SI(x)** connects **n-1** lines is twice as high as the probability that the same defect connects **n** lines. Also, the probability that a defect connecting **n** lines has a size within the size interval **SI(x+1)** is twice as high as the probability that the same defect has a size within the size interval **SI(x)**. So, **α(n)** will be calculated as

$$\alpha(n) := \frac{1}{3}\cdot d(n) \tag{12}$$

For **n≥1**, **β(n)** will be calculated as

$$\beta(n) := \begin{cases} 0 & \text{if} \quad n = 1 \\ \frac{2}{3}\cdot d(n) & \text{if} \quad n \geq 2 \end{cases} \tag{13}$$

5 Experimental Results

At ELMOS in Dortmund, Germany, a harp test structure was manufactured to control defect appearance in a 2-metal layer interconnection process. The HTS has 466 permuted horizontal test structure lines in the metal-1 layer. The metal-2 layer contains 352 permuted vertical test structure lines. Figure 14 shows the upper left corner of the manufactured HTS. The complete harp test structure design can be seen in Figure 10. It just takes a few seconds to automatically generate the harp test structure. The Figures 11, 12, and 13 show defects connecting different numbers of adjacent harp lines.

Fig. 10: Design of a 2-metal harp test structure containing 818 test structure lines in 2 interconnection layers.

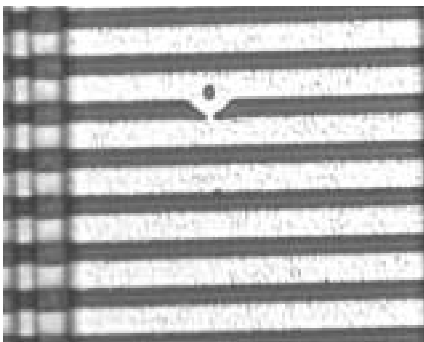

Fig. 11: Detected defect that connects 2 lines.

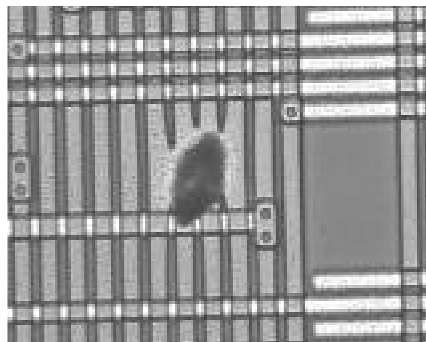

Fig. 12: Detected defect that connects 4 lines in a routing channel.

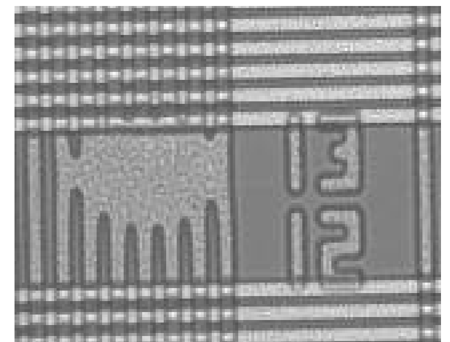

Fig. 13: Detected defect that connects 7 lines.

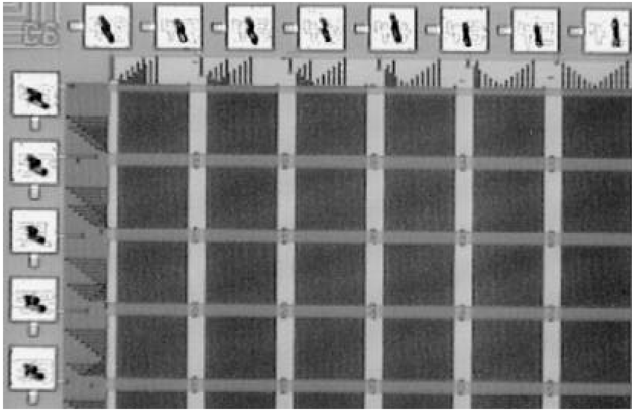

Fig. 14: Harp test structure manufactured at ELMOS in Germany.

If defects occur and cause a fault, adjacent harp lines are connected to each other. Since we know which test structure lines are adjacently implemented, we can conclude to the harp bundle and the line indices to position the defects. The following Figures 15 and 16 give the defect size distributions using the methodology to analyze electrically measured data (ref. Section 4).

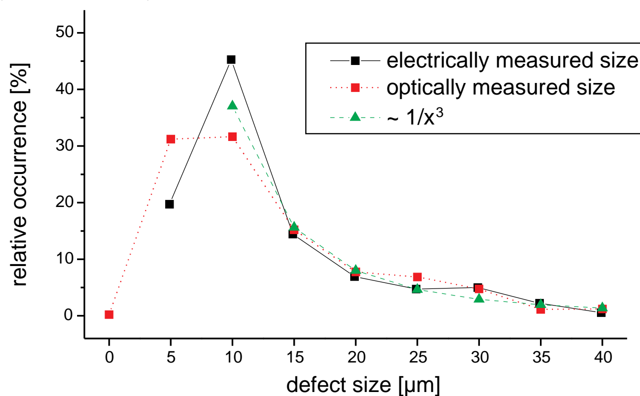

Fig. 15: Comparison of defect size distributions in lot "A" of 23 wafers, each containing 109 harp test structures.

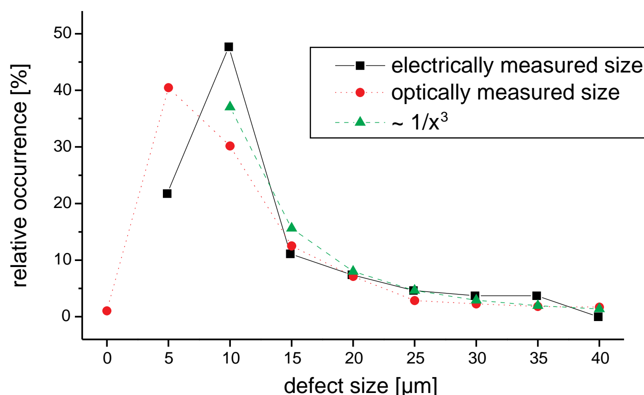

Fig. 16: Comparison of defect size distributions in lot "B" of 25 wafers, each containing 109 harp test structures.

We also took photos of all electrically detected defects, which was possible because of the defect localization procedure described in Section 3. So, the Figures 15 and 16 also contain size distributions based on optical measurements using a technic called *micro size distribution (MSD)*, which was introduced by [HeWe96b]. If defects connect more than 3 harp lines, electrical measurements at a harp test structure are sufficient to get a precise defect size distribution that fits to known analytical distributions (e. g. $\sim 1/x^3$ at [StRo95]). Keep in mind that the electrically based measurement procedure just needs a fraction of the time which is necessary to optically analyze defect pictures.

6 Conclusion

The described method to place test structure lines inside a given pad frame enables an efficient inspection of defects that occur in any layer. The harp test structure detects systematic problems as well as random defects due to its extensive defect sensitive area. However, the permutation of test structure lines guarantees a precise separation of digitally measured single and multiple faults. Furthermore, layer-specific defects will be extracted from each detected fault to determine defect densities and size distributions based on electrical measurements only. The systematical design of the harp test structure enables a machine-assisted generation of test chips. There is no limitation to the number of layers and no requirement of any active semiconductor devices to separate test structure lines or disentangle multiple faults, respectively.

Acknowledgment

Parts of this research were supported by *Deutsche Forschungsgemeinschaft* (DFG), Schm623/3. The authors thank R. Bornefeld, M. Prott and C. Strauch (ELMOS, Dortmund, Germany) for advice and assistance with manufacturing and testing procedures.

References

[BCKJ91] Bruls, E. M. J. G., Camerik, F., Kretschman, H. J., Jess, J. A. G. A
Generic Method to Develop A Defect Monitoring System for IC Processes
International Test Conference, 1991

[Ferr85c] Ferris Prabhu, A. V.
Role of Defect Size Distribution in Yield Modeling
IEEE Transactions on Electron Devices, Vol. ED-32, No. 9, 1985

[HeSt94] Hess, C., Ströle, A.
Modeling of Real Defect Outlines and Defect Parameter Extraction Using a Checkerboard Test Structure to Localize Defects
IEEE Transactions on Semiconductor Manufacturing, Vol. 7, No. 3, 1994

[HeWe96b] Hess, C., Weiland, L. H.
Issues on the Size and Outline of Killer Defects and their Influence on Yield Modeling
Proc. Advanced Semiconductor Manufacturing Conference, Boston, 1996

[HWLH96] Hess, C., Weiland, L. H., Lau, G., Hiller, R.
Correlation Between Particle Defects and Electrical Faults Determined with Laser Scattering Systems and Digital Measurements on Checkerboard Test Structures
Proc. 1996 SPIE's Microelectronic Manufacturing, Austin (USA), 1996

[Maly90] Maly, W.
Computer-Aided Design for VLSI Circuit Manufacturability
Proceedings of the IEEE, Vol 78, No. 2, Feb. 1990

[Stap84] Stapper, C. H.
Modeling of Defects in Integrated Circuits Photolithographic Patterns
IBM J. Res. Develop., Vol. 28, No. 4, July 1984

[StRo95] Staper, C. H., Rosner, R. J.
Integrated Circuit Yield Management and Yield Analysis: Development and Implementation
IEEE Transactions on Semiconductor Manufacturing, Vol. 8, No. 2, 1995

[TBG95] Trafas, B. M., Bennett, M. H., Godwin, M.
Meeting Advanced Pattern Inspection System Requirements for 0.25µ Technology and Beyond
Proc. 1995 SPIE's Microelectronic Manufacturing: Yield, Reliability, and Failure Analysis, Spie Vol. 2635, Austin (USA), 1995